

# Computer graphic modelling in drug design: conformational analysis of dihydrofolate reductase inhibitors

V Cody

Research Laboratories, Medical Foundation of Buffalo Inc., 73 High Street, Buffalo, New York 14203, USA

*Lipophilic 2,4-diaminopyrimidines with a 5-adamantyl substituent are effective inhibitors of mammalian dihydrofolate reductase (DHFR) and produce an additional 1 000-fold increase in their cytotoxic activity when the substituent in position six is changed from hydrogen to ethyl, but drops at propyl. The results of X-ray crystal structure analysis of these antifolates show that the pyrimidine ring and its substituents become more distorted from coplanarity as the size of the 6-substituent increases. Computer graphic modelling of the binding of these antifolates in the active site of the chicken liver DHFR-NADPH binary complex indicates that both the adamantyl group and 6-substituent occupy hydrophobic pockets. Exploration of the size and character of the protein environment about the 6-position suggests that neither the ethyl nor the propyl group make optimal contacts with the functional groups surrounding this pocket. From these studies the design of alternative 6-substituent antifolates are suggested which could make specific contacts with the residues in this region of the protein.*

**Keywords:** drug design, computer graphic modelling, dihydrofolate reductase inhibitors

The enzyme dihydrofolate reductase (DHFR), a necessary component for all cell growth, is strongly and specifically inhibited by certain substrate analogues with binding affinities so great that they are not readily displaced by the natural folic acid substrates. These antifolates have been the focus for the chemotherapy of infectious and neoplastic diseases because of their ability to interfere with the conversion of folic acid and dihydrofolic acid to tetrahydrofolic acid. This inhibition causes the depletion of N5,N10-methylenetetrahydrofolic acid which is a necessary cofactor in the synthesis of purine and pyrimidine nucleotide precursors of DNA and RNA<sup>1-5</sup>. Many of these antifolates have an inhibitory action which is specific for different species of DHFR. Figure 1 shows that the most widely used anticancer drug methotrexate (MTX) is homologous with the natural folic acid substrate. However, the change in substrate composition from 4-keto to 4-amino modifies the reso-

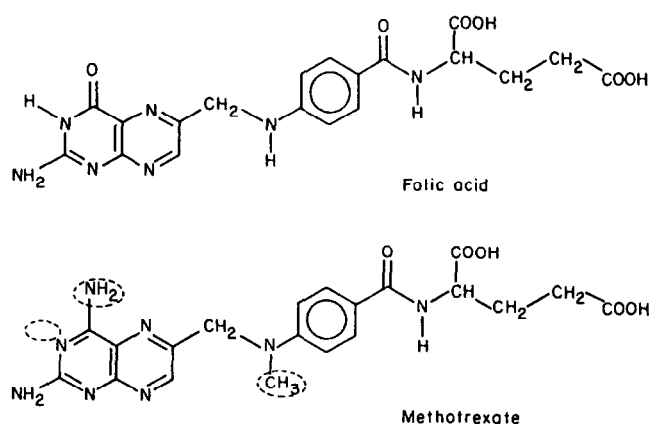


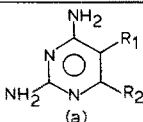
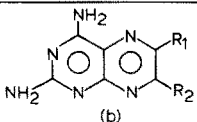
Figure 1. Comparison of the natural DHFR substrate folic acid (a) and anticancer chemotherapeutic inhibitor methotrexate (b)

nance structure of the amino pteridine ring which in turn changes its solubility and basicity, as well as the ease of protonation of the pteridine ring. Binding affinity data show that MTX is more tightly bound to DHFR when protonated at N1, whereas folic acid binds best as a neutral species<sup>2-4</sup>.

It has been demonstrated that the principal structural characteristic necessary for tight binding to DHFR from any species is a 2,4-diamino pyrimidine, s-triazine, or pterine ring structure<sup>1-6</sup>. Structure-activity studies of 2,4-diaminopyrimidines indicate that a lipophilic group at position five is also essential for tight binding to DHFR. Marked differences in the inhibitory potency have been observed concomitant with small changes in the chemical structures of these antifolate drugs. Comparison of several lipophilic antifolates shows that those with a 5-adamantyl substituent are the most effective inhibitors of mammalian DHFR with potencies greater than MTX (see Table 1)<sup>6-9</sup>. These structures have greater binding affinities for DHFR than those with comparable molar volume and hydrophobicity<sup>7,8</sup>. Furthermore, these adamantyl antifolates have cellular uptake rates about 10 000 times more rapid than methotrexate, and show strong cytotoxic activity in culture cells<sup>10</sup>.

X-ray crystallographic analyses were carried out on

**Table 1. Lipophilic 2,4-diaminopyrimidine inhibitors of DHFR**

 (a)		 (b)	
(a) R <sup>1</sup>	R <sup>2</sup>	Structure <sup>a</sup>	ID <sub>50</sub> M <sup>b</sup>
adamantyl	propyl	DAPP	4.8 × 10 <sup>-8</sup>
adamantyl	ethyl	DAEP	2.5 × 10 <sup>-10</sup>
adamantyl	methyl	DAMP	6.0 × 10 <sup>-9</sup>
adamantyl	hydrogen	DAHP	3.3 × 10 <sup>-7</sup>
cyclohexyl	methyl	DCXMP	3.9 × 10 <sup>-7</sup>
heptyl	methyl	DHMP	1.6 × 10 <sup>-6</sup>
t-butyl	methyl	DTMP	1.9 × 10 <sup>-5</sup>
1-naphthyl	methyl	DNMP-1	5.6 × 10 <sup>-4</sup>
2-naphthyl	methyl		7.0 × 10 <sup>-8</sup>
(b) R <sup>1</sup>			
p-aminobenzoylglutamate		MTX	8.0 × 10 <sup>-6</sup>
adamantyl		Dapt	1.4 × 10 <sup>-7</sup>
	R <sup>2</sup>		
	adamantyl		4.8 × 10 <sup>-6</sup>

<sup>a</sup>These are names assigned to the crystal structures of these compounds, e.g., DAMP is DiaminoAdamantyl-MethylPyrimidine

<sup>b</sup>50 % growth inhibition of mouse mammary adenocarcinoma cells (TA3) in culture<sup>7</sup>

a number of 5(1-adamantyl) lipophilic antifolates (see Figure 2) in order to delineate their conformational and electronic properties, and the structural features which are important for their species specificity and selectivity. In addition, computer graphic modelling of the binding interactions of these antifolates within the active site of chicken liver dihydrofolate reductase were investigated<sup>11-17</sup>

These studies revealed that within the series of 6-substituted diaminoadamantyl-pyrimidines (DAMP, DAEP, DAPP, DAHP), the pyrimidine ring in each structure is distorted from coplanarity with its substituents, while that of the 6-H (DAHP) analogue is planar. As a result of the steric strain placed upon the system by the close intramolecular interactions of the adamantyl hydrogen atoms and those of the 4,6-substituents (see Table 2), the pyrimidine ring is distorted from planarity, it becomes a flattened boat with C2 and C5 above the N1,N3,C4,C6 plane. In some structures the adamantyl group is as much as 0.46Å from this plane (see Table 3) and result in an overall bowing of these antifolates (Figure 3).

The structure of the 5-t-butyl analogue (Table 1, DTMP) was investigated to explore the influence of a tertiary carbon substituent at position 5. The structure of DTMP reveals that the pyrimidine ring is planar and both the 5-t-butyl and 6-methyl carbon atoms are disordered. This observation suggests that the t-butyl group is flexible and can relieve the strain associated with the proximity of the 4,6-substituent hydrogen atoms. In the case of the 5-(1-adamantyl) antifolates, the rigidity of the adamantyl ring forces the molecule to absorb the steric strain in the disruption of the pyrimidine ring from planarity<sup>13</sup>.

The pyrimidine ring of the 5-cyclohexyl and 5-(1-naphthyl) analogues (Table 1: DCXMP, DNMP-1) are also planar. As demonstrated, the inhibitory potency

of DCXMP is the same as DAHP, suggesting that the hydrophobic and lipophilic effects on binding affinity of the 5-cyclohexyl-6-methyl are comparable to those of the 5-adamantyl-6-H. The lower potency of DTMP suggests that the size of the t-butyl group is such that its contribution to hydrophobic binding is too small. Although the crystal structure of the 5-(2-naphthyl) analogue has not been determined, comparison with the 5-(1-naphthyl) analogue, suggests that it would have a similar structure. The extremely low potency in this system suggests that there are severe steric constraints prevent its binding to DHFR<sup>7</sup>.

The structures of pteridine antifolates were also investigated (see Table 1) and their properties compared with MTX and the pyrimidine structures<sup>18,19</sup>. Structure-activity data for the adamantyl pteridine analogues show that the inhibitory potency of the 6-adamantyl analogue is comparable to MTX, while its 7-adamantyl isomer is lower (see Table 1)<sup>20</sup>. However, when the structure of the 6-adamantyl analogue was determined, it proved to be that of the 6-adamantyl folate<sup>18</sup>, indicating oxidation at the C4 position. Figure 4 shows the overall shape of the pteridine and pyrimidine adamantyl analogues is similar. However, there are differences in their structural homology which are of importance to their binding at the DHFR active site. If the adamantyl groups are matched (see Figure 5a), the diamino functions are no homologous. Similarly, if the diamino functions are matched, the bulk of the adamantyl rings occupy different spatial orientations (see Figure 5b).

## HYDROGEN BONDING INTERACTIONS

The high affinity of antifolates for the enzyme active site is assumed to involve strong multiple hydrogen bonding interactions<sup>6</sup>. Examination of intermolecular interactions in the solid state reveals the characteristic formation of N...N base-pair hydrogen bonds involving N4 hydrogen donation to N3 of an adjacent molecule. This in turn donates its N4 hydrogen to N3 of the first molecule (see Figure 6). This is a preferred pattern. In most instances, the base-pair is symmetric because it occurs around an inversion centre in the crystal lattice. However, this pattern is also found in the structure of DAEP<sup>13</sup>, which has no crystallographic constraints.

Comparison of average geometric parameters of 11 pyrimidine rings protonated at N1 with 17 unprotonated at N1 reveals characteristic differences (see Figure 7) that undoubtedly effect the hydrogen bond strength of the other nitrogen substituents. This data also indicates considerable double bond character in the exocyclic nitrogen bonds as the exocyclic C-N bond distances are shorter than those found in other aromatic diamino compounds<sup>16</sup>.

## DHFR ENZYME-INHIBITOR BINDING MODELS

Precise crystallographic data delineating the DHFR enzyme structure and inhibitor/cofactor complexes are available from two bacterial and one avian species<sup>21-23</sup>. This data shows that the active site is located within a 15Å cavity cutting across one face of the enzyme and is lined by hydrophobic side chains<sup>2,21-23</sup> and further indicate that MTX binds to the enzyme in an open conformation with the pteridine ring nearly perpendicular to the benzoyl ring (see Colour Plate 1). Structural data

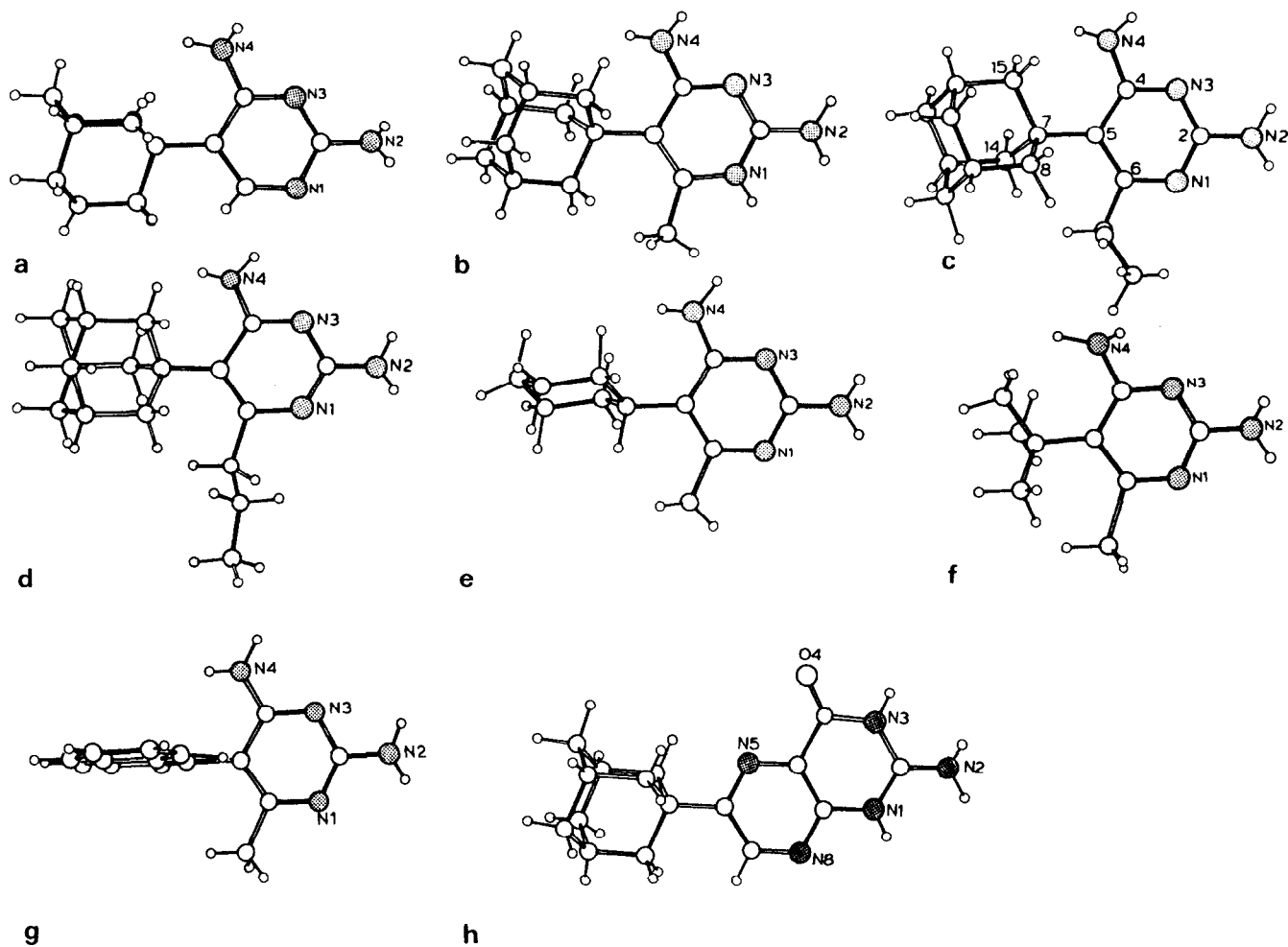


Figure 2. Molecular conformations of (a) DAHP, (b) DAMP, (c) DAEP, (d) DAPP, (e) DCXMP, (f) DTMP, (g) DNMP-1 and (h) DApt

Table 2. Closest nonbonded H...H intramolecular contacts for 4,6-substituents (All values in Å)

Contact	DAHP	DAMP	DAEP	DAPP
H61A ...	H8B 2.09 <sup>a</sup>	H8A 2.06	H8A 1.82	H15B 3.24
B ...		H8A 3.39	H14B 2.69	H15B 1.66
C ...		H8B 2.14		
H62A ...			H8A 2.80	H15 1.99
B ...			H9A 3.85	H15B 3.34
C ...			H8A 4.13	
H4A ...	H12B 2.12	H14A 2.98	H15A 3.20	H8A 1.89
B ...	H13B 2.16	H15B 1.88	H15A 1.83	

<sup>a</sup>Only those values < 2.00 Å are significant

Table 3. Deviations of 2,4,5,6,7-Substituents from N1,N3,C4,C6 plane (All measurements in Å)

Substituent	DAHP	DAMP	DAEP	DAPP
N2	0.037	-0.234	-0.254	-0.329
N4	-0.036	0.236	0.241	0.366
C7	-0.039	-0.419	-0.461	-0.431
C61	-0.157	-0.054	0.418	0.232
C2	0.009	-0.088	-0.087	-0.155
C5	0.024	-0.121	-0.122	-0.165

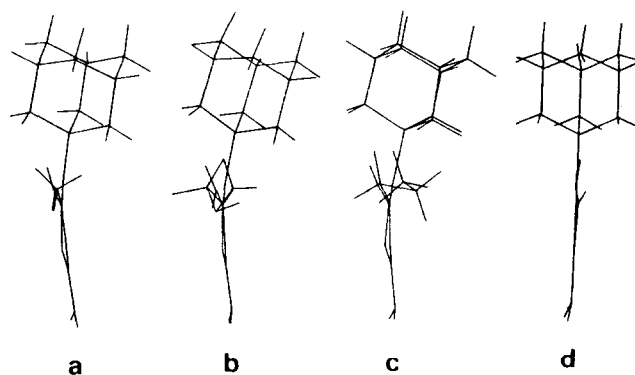


Figure 3. Comparison of the bowed shape of (a): DAMP; (b): DAEP; (c): DAPP; and (d): planar DAHP

shows that DAMP also binds to chicken liver DHFR with its diaminopyrimidine ring in the same location as the pteridine ring diaminopyrimidine moiety (see Colour Plate 2).<sup>23</sup>

Modelling studies illustrating the binding of these antifolates (Table 1) to the active site in the chicken liver DHFR-NADPH binary complex were carried out at the University of California, San Francisco, using MIDAS on their computer graphics system<sup>24</sup>. In each case, the pyrimidine ring was matched to that of DAMP in the active site of the chicken liver DHFR-NADPH-DAMP

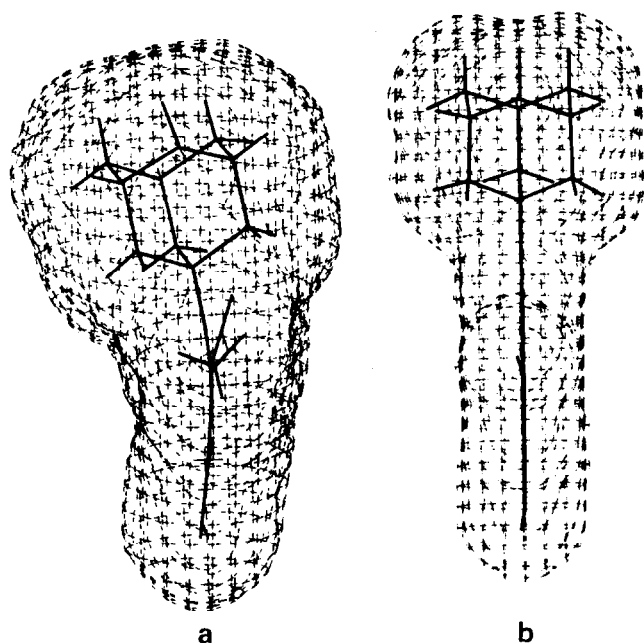


Figure 4. Comparison of the molecular volumes of (a): DAMP; and (b): DApT, projected parallel to their diamino ring planes

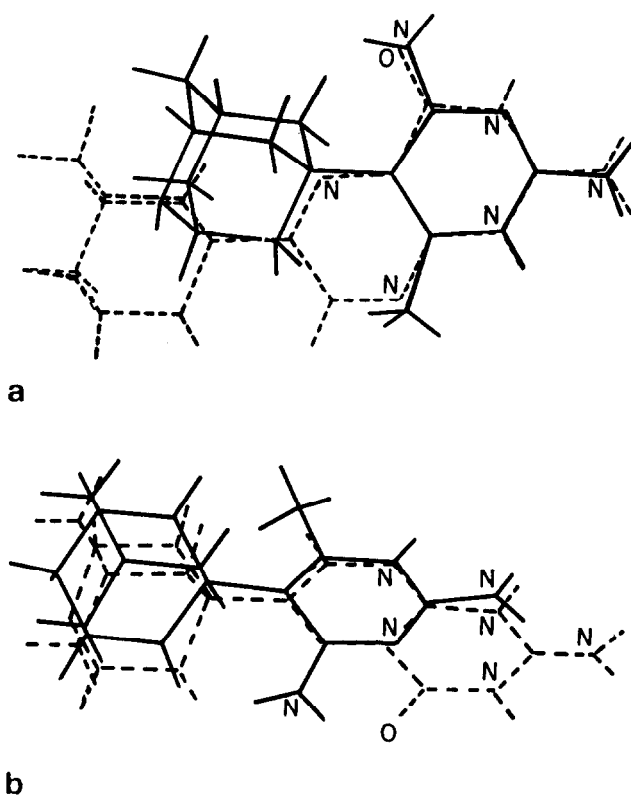


Figure 5. Molecular conformation of DApT and DAMP (a) with their diaminopyrimidine rings superimposed, and (b) with their adamantyl rings superimposed

ternary complex and the molecular interactions of the antifolate with the enzyme residues investigated.

When the interactions of DAMP in the chicken liver DHFR active site are modelled it is shown that the adamantyl ring fits tightly into the hydrophobic pocket near that occupied by the *p*-aminobenzoyl ring (Colour Plate 3). These studies further show that the 6-methyl-

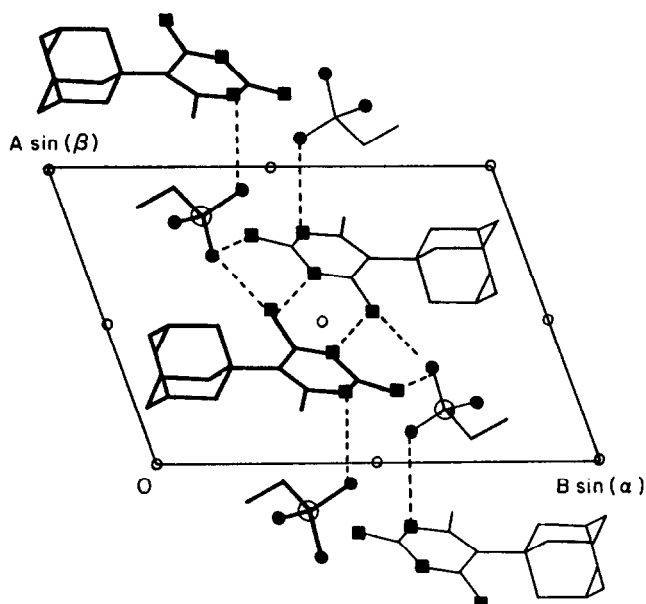


Figure 6. Typical hydrogen bonding pattern observed for 2,4-diaminopyrimidine antifolates as demonstrated by the structure of DAMP ethanesulphonate<sup>11</sup>

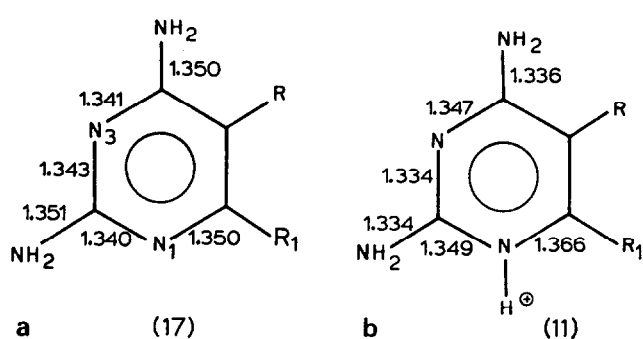


Figure 7. Comparison of the average diaminopyrimidine geometries calculated from the crystal structure analysis of N1 (a) unprotonated (No. of structures = 17) and (b) protonated antifolates (No. of structures = 11)

group is also in a hydrophobic pocket formed by the residues Trp-24, Glu-30 and Tyr-31.

To explain the large differences in the inhibitory potencies of the 5-(1-naphthyl) and 5-(2-naphthyl) analogues, their binding was investigated. Colour Plate 4a shows that the 1-naphthyl ring cuts through the enzyme surface. Rotation about the naphthyl-pyrimidine ring bond does not relieve any of these steric interactions<sup>11</sup>. However, when the 2-naphthyl analogue is placed in the active site there are no steric interactions (see Colour Plate 4b). These observations suggest that steric interference of the 1-naphthyl ring is the reason for its inactivity even though it has the same lipophilicity and hydrophobicity as the 2-naphthyl analogue.

One of the most striking features of the DAEP binding model is shown in Colour Plate 5. Colour Plate 5a shows the 6-ethyl environment with DAEP in its crystallographically observed conformation. A 110° rotation of the ethyl side chain (shown in Colour Plate 5b) (also a stable and assessible conformation) places the ethyl group into what appears to be a more suitable pocket. A similar comparison of the fit of the 6-propyl side

chain (see Colour Plate 6), indicates that it can also fit into this space. In its crystallographic orientation, the propyl side chain C63 is 2.38Å from the hydroxy oxygen of Tyr-31 (see Colour Plate 6a). A 60° rotation of the side chain, (similar to that carried out with DAEP) increases this distance to 3.64Å (see Colour Plate 6b).

These observations suggest that other 6-substituted pyrimidine antifolates can be suggested which could take advantage of specific interactions with these residues. Accordingly, computer generated models were made for other 6-substituted diaminoadamantylpyrimidines and their fit tested in this pocket. For example, if a 6-acetoxy group were placed in this region, its O ... O contact distance to Tyr-31 is 3.30Å, a favourable hydrogen bonding distance (see Colour Plate 7). This modelling study implies that a more potent lipophilic antifolate could be developed which could make specific contacts to the enzyme residues. Similar studies have been carried out with the antibacterial trimethoprim binding in bacterial DHFR<sup>3,4</sup>.

While these studies did not satisfactorily explain the difference in potencies between DAEP and DAPP, they did suggest the synthesis of other, perhaps more potent, antifolates which could maintain the inhibitory properties of these adamantyl antifolates. These modelling studies suggest that other parameters are of importance to the binding affinity of these adamantyl compounds which could explain better the maximal potency of DAEP in this series. Another factor is that the avian active site does not properly reflect the true nature of mammalian DHFR species. The synthesis and testing of these new model antifolates will shed light on the significance of these modelling procedures. Such studies are currently underway.

## ACKNOWLEDGEMENTS

This research was supported in part by grants from the NCI-34714, an American Cancer Society Faculty Research Award, FRA-287, and the Buffalo Foundation. The author wishes to thank the staff at UCSF Computer graphics laboratory for their help, Dr David Matthews for making available his coordinates of chicken liver DHFR, and Dr Paul Sutton, Melda Tugac and Gloria Del Bel, for their technical assistance.

## REFERENCES

- 1 Hitching, G H and Burchall, J J *Adv. Enzymol.* Vol 27 (1965) pp 417–468
- 2 Blakley, R L in Blakley, R L and Benkovic, S J (Eds) *Folates and Pterins*, Vol 1 (1984) John Wiley & Sons, New York, pp 191–253
- 3 Roth, B and Cheng, C C *Progr. Medicinal Chem.* Vol 19 (1982) pp 270–331
- 4 Blaney, J M, Hansch, C, Silipo, C and Vittoria, A *Chem. Rev.* Vol 84 (1984) pp 333–407
- 5 Burchall, J J and Hitching, G H *Mol. Pharmacol.* Vol 1 (1965) pp 126–136
- 6 Zakrzewski, S F *J. Biol. Chem.* Vol 238 (1963) pp 1485–1490; pp 4002–4004
- 7 Jonak, J P, Zakrzewski, S F, and Mead, L H *J. Med. Chem.* Vol 14 (1971) pp 408–411; *J. Med. Chem.* Vol 15 (1972) pp 662–665
- 8 Kawai, I, Mead, L H, Drobnik, J and Zakrzewski, S F *J. Med. Chem.* Vol 18 (1975) pp 272–275
- 9 Zakrzewski, S F, Dave, C and Rosen F J *Natl. Cancer Inst.* Vol 60 (1978) pp 1029–1033
- 10 Greco, W R and Hakala, M T *Mol. Pharmacol.* Vol 18 (1980) pp 521–528
- 11 Cody, V and Zakrzewski, S F *J. Med. Chem.* Vol 25 (1982) pp 427–431
- 12 Cody, V, Welsh, W J, Opitz, S and Zakrzewski, S F in Kuchar, M (Ed) *QSAR in Design of Bioactive Compounds*, J R Prous Science, Barcelona, Spain (1984) pp 241–252
- 13 Cody, V in Rein R (Ed) *Molecular Basis of Cancer, Part B: Macromolecular Recognition, Chemotherapy and Immunology* Alan R. Liss, Inc. New York (1984) pp 275–284
- 14 Cody, V, DeJarnette, E and Zakrzewski, S F in Blair, J A (Ed) *Chemistry and Biology of Pteridines* de Gruyter, Berlin (1983) pp 293–297
- 15 Welsh, W J, Mark, J E, Cody, V and Zakrzewski, S F in Blair, J A (Ed) *Chemistry and Biology of Pteridines* de Gruyter, Berlin (1983) pp 463–468
- 16 Schwalbe, C H and Cody, V in Blair, J A (Ed) *Chemistry and Biology of Pteridines* de Gruyter, Berlin (1983) pp 511–515
- 17 Welsh, W J, Cody, V, Mark, J E and Zakrzewski, S F *Cancer Biochem. Biophys.* Vol 7 (1983) pp 27–38
- 18 Cody, V, Opitz, S and Zakrzewski, S F *Fed. Proc.* Vol 43 (1984) p 1730
- 19 Sutton, P A, Cody, V and Smith G D, in preparation
- 20 Jonak, J P, Zakrzewski, S F, Mead, L H and Allshouse, L D *J. Med. Chem.* Vol 15 (1972) pp 1331–1332
- 21 Bolin, J T, Filman, D J, Matthews, D A, Hamlin R C, and Kraut, J *J. Biol. Chem.* Vol 257 (1982), pp 13650–13662
- 22 Matthews, D A, Bolin J T, Burridge J M, Filman, D J, Volz, K W, Kaufman B T, Beddell, C R, Champness, J N, Stammers, D K and Kraut, J *J. Biol. Chem.* Vol 260 (1985) pp 381–391
- 23 Matthews, D A, Bolin, J T, Burridge J M, Filman, D J, Volz, K W and Kraut J *J. Biol. Chem.* Vol 260 (1985) pp 392–399
- 24 Langridge, R, Ferrin, T E, Kutz, I D and Conolly, M, *Science* Vol 211 (1981) pp 661–666